The Floating PML Applied to Practical FDTD Applications

M. Wong and A. R. Sebak

Concordia University, Montreal, Quebec
mich_won@ece.concordia.ca

Abstract – In this paper we present the Floating Perfectly Matched Layer (Floating PML) where a "floating" PML is implemented within the solution space without making contact with the main PML walls. The Floating PML can be used as a terminating technique within the solution space of the Finite Difference Time Domain (FDTD) Method. The formulation of the Floating PML is based on an optimized implementation of the Convolutional PML (CPML), which is discussed briefly in the Appendix. In this paper we present benchmark validation tests, applications using the Floating PML, as well as some advantages and disadvantages of this method.

I. INTRODUCTION

The Finite Difference Time Domain (FDTD) method is an extremely versatile, simple computational tool that has been used extensively in recent applications involving electromagnetics [1, 2]. In general, the FDTD method requires the truncation of the solution space so that an infinitely large solution space is not required to simulate free space. This problem of terminating the solution space has been an important component in the development of the FDTD method, and continues to be an area of active research [3].

When investigating various transmission line structures such as microstrips, striplines, or waveguides, it is convenient to terminate the line at the edge of the solution space. This is a common terminating technique as shown in Fig. 1 [2, 4]. This type of port is often used because the termination of a transmission line in a PML, which simulates an infinitely long transmission line, is very convenient to implement in the FDTD method and ensures a very low return loss which does not interfere with the analysis of the structure itself.

It is, however, often necessary to terminate the transmission line within the solution space instead of at its edge. This type of termination, often called a port, is used so that the entire structure may be simulated without any contact to any Absorbing Boundary Condition (ABC) or Perfectly Matched Layer (PML) at the edge of the solution space. This is necessary so that a radiation box may surround the structure to perform a near to far field operation, so that the finite size of a device may be taken into account during a simulation, or so that the port itself may be surrounded by other devices. An example of this is shown in Fig. 2.

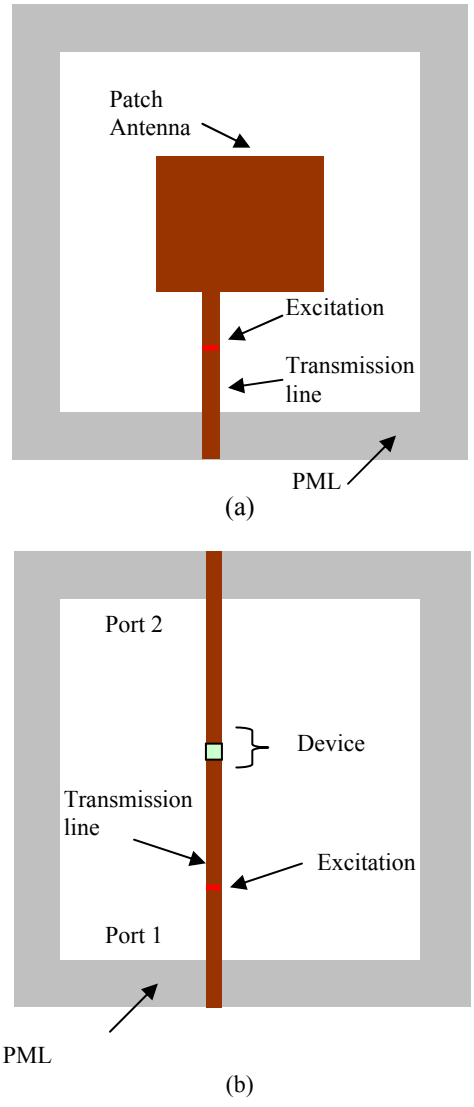

Fig. 1. Common terminating techniques applied to FDTD, (a) microstrip patch antenna [4] with a transmission line terminated in the PML and (b) circuit modeling for arbitrary lumped elements (Device) using the main PML for termination of the 2 ports [2].

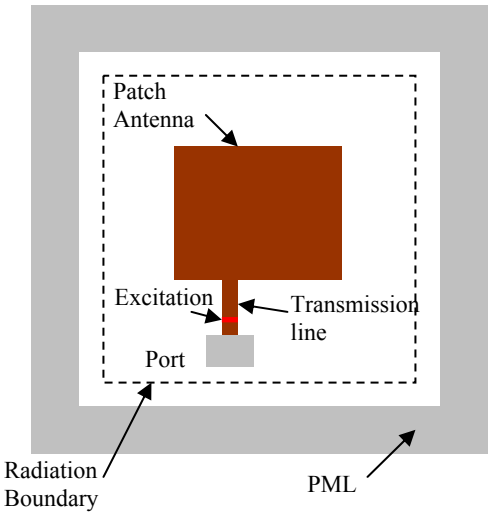

(a)

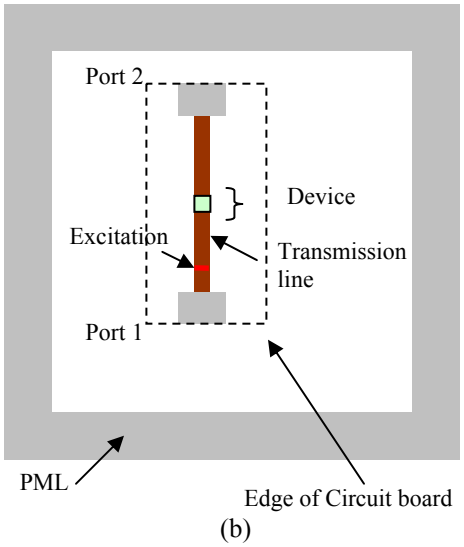

(b)

Fig. 2. Terminating technique when (a) a radiation pattern must be found and (b) finite ground plane of a circuit must be taken into account.

Various techniques have been reported for implementing a port within the solution space. Luebbers and Langdon [5] have implemented a resistive source, and Schuster and Luebbers have terminated transmission lines with lumped loads [6] using a recursive convolution technique. Piket-May and Taflove [7] have implemented similar loads, however, their results show that the resistor generates parasitic capacitance at frequencies above 1 GHz. Recently, the Lumped Element FDTD Method has been introduced which can model high-speed microwave circuit networks consisting of active and passive devices within a single Yee cell [2, 8]. This type of element can also be used to simulate a port within the solution space.

In this paper we present an alternative approach which implements the termination of a port using a PML within the solution space [9] away from the main PML wall. In some cases we may prefer to model a port as an infinitely long transmission line within the solution space, as opposed to a lumped element attached to a transmission line. To achieve this, we introduce an optimized Convolutional Perfectly Matched Layer (CPML) formulation that fully separates PML equations from FDTD equations, as discussed in the Appendix. Adding the PML within the solution space then becomes simple and very useful. This technique is referred to as the Floating PML [9], since this PML does not touch the external walls of the solution space and can therefore act as a port. This method results in a wideband operation with low radiation losses where results are discussed in the following sections.

We begin with the discussion of the Floating PML and describe its "physical" structure. Benchmark tests are then performed, followed by examples of practical electromagnetic applications. The optimized CPML formulation is included in Appendix A.

II. INTRODUCING THE FLOATING PML

As discussed in the introduction, there exist various methods to terminate a port using a resistor or lumped elements within the solution space, however, the Floating PML provides wideband characteristics simply by the nature of its structure since it models an infinitely long transmission line.

In addition, some methods such as microstrip termination using the resistive voltage source suffer from parasitic capacitance above 1 GHz [7]. This limits its potential for use at high frequencies. The Floating PML described in this section is extremely wideband by comparison and is perhaps a better choice for higher frequencies.

The PML in a regular solution space is typically surrounded by metallic walls [3] as shown in Fig. 3. This technique ensures a "double" attenuation of incoming waves, since they are attenuated as the hit the PML, and attenuated again as they are reflected. The Floating PML is implemented in a similar way, that is, with a metallic box surrounding the PML. It was found that for this implementation of the Floating PML, the PEC box was required to maintain stability of the solution space.

During simulations of microstrip and stripline structures, it was found that it is best to model the PEC box with a transmission line as a rectangular coaxial cable as discussed in [11]. Using this model, it is possible to model the PEC walls at a distance large enough to avoid interaction with the transmission line.

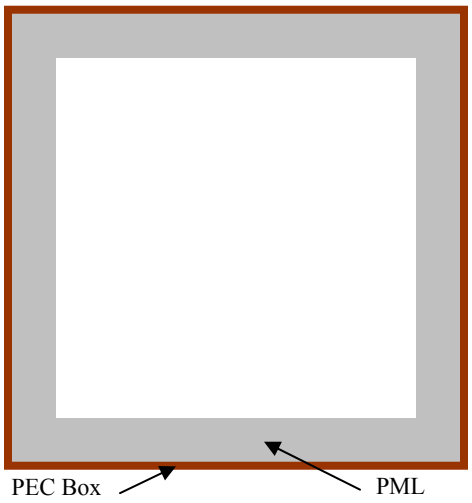

(a)

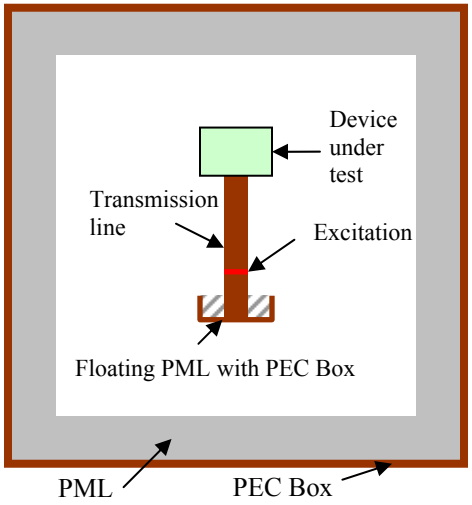

(b)

Fig. 3. Use of a PEC box in (a) the main PML wall in a typical solution space and (b) with the floating PML, modeled as a rectangular coaxial cable [11].

There are some advantages and disadvantages of the Floating PML as a terminating technique. One disadvantage is that the PEC box will affect the simulation, however, this box is not more intrusive than an SMA connector used during real measurements. The PEC box has the advantage that there are very low radiation losses at the port compared to resistive loads. An additional advantage is that the PEC box is well suited to waveguide applications. The Floating PML is extremely wideband simply by the nature of the structure itself because the port is modeled as an infinitely long transmission line. One problem that was encountered during simulation was that the Floating PML did not perform as well for microstrip terminations as for stripline terminations as is discussed in the following sections in this paper. Finally, the Floating PML is very easy to implement using the optimized CPML formulation discussed in the Appendix, however, requires more computational resources than a resistive source.

III. BENCHMARK PERFORMANCE OF THE FLOATING PML

In this section we measure the return loss performance of the Floating PML over a large frequency range from 0 to 20 GHz. A good return loss indicates that the port absorbs most of the incoming waves, thus not interfering with reflected waves from the simulated structure.

A. Stripline Applications

In this example, we examine a stripline structure that terminates in the PML wall on one side, and in the Floating PML on the other side as shown in Fig. 4. In this test, we attempt to attain the lowest possible return loss for a Gaussian incident pulse on the Floating PML.

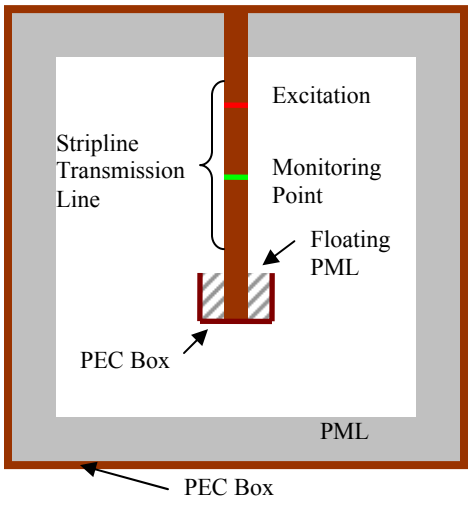

Fig. 4. Structure for the benchmark test for the stripline transmission line incident on the floating PML.

For the test as shown in Figs. 4 and 5, we have run various widths for the PEC box. It was found that a larger width of box provided fewer reflections.

In Fig. 6 we show that the return loss for the stripline incident on the Floating PML has a very wideband performance with a return loss of better than 50 dB from 0 GHz to 20 GHz. The number of cells represents the distance from the PEC box to the trace.

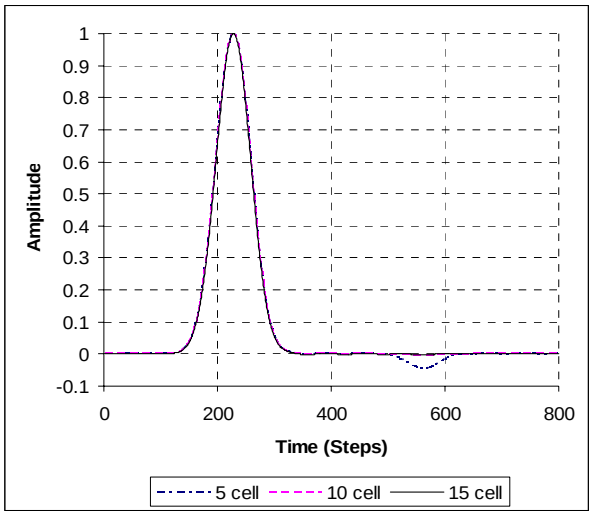

Fig. 5. Time-domain simulation for various widths of the PEC box. The number of cells represents distance on either side of the transmission line between the line and the PEC wall. Each cell is 0.2 mm large.

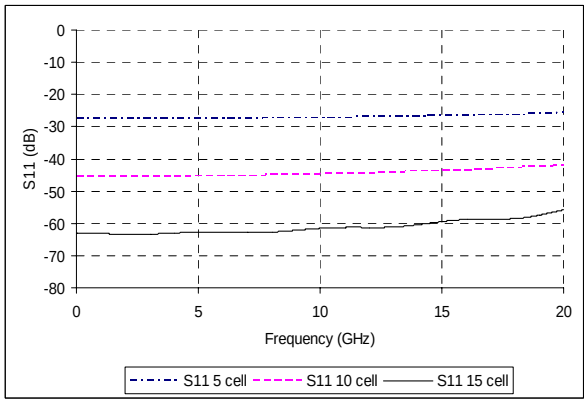

Fig. 6. Return loss for the stripline incident on the floating PML for differently sized PEC boxes.

B. Microstrip Applications

In this section we examine a microstrip transmission line terminating in a Floating PML as shown in Fig. 7. The transmission line is 1.88 mm wide and lies on a 0.813 mm thick Rogers 5880 substrate, with a dielectric constant of 3.38. The Floating PML consists of the PML material surrounded by a PEC box. The bottom half of the box is filled with the Rogers 5880 substrate, while the top half of the box is filled with air.

In this method, the PEC box is made large enough to reduce the interaction of the fields traveling along the microstrip line with the PEC box. The size of the cells is 0.31374 mm wide in the x and y directions, and 0.20325 mm tall in the z direction.

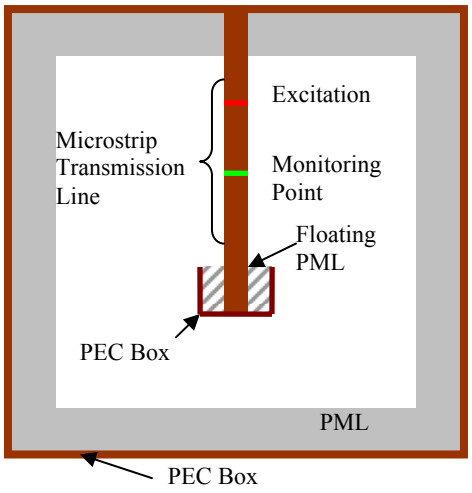

Fig. 7. Structure for the benchmark test of a microstrip transmission line incident on a floating PML. The top half of the floating PML box is filled with air. The bottom half is filled with the same dielectric as the substrate. The whole floating PML box is filled with PML material.

In Fig. 8. we have simulated various sizes for the PEC box. It was found that a larger box provided a fewer reflections. The number of cells represents the distance from the trace in both the x and z directions.

In Fig. 9. we show that for a larger PEC box, the return loss is improved. This correlates with the fewer reflections seen in Fig. 8. The performance for the microstrip case is not as good as for the stripline case because of the difference in dielectric constant throughout the Floating PML.

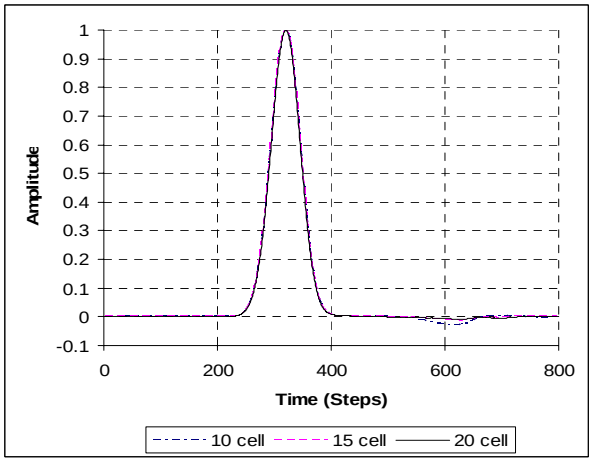

Fig. 8. Time domain comparison of Floating PML. The incident wave is clearly visible while the reflected wave is barely visible around 600th time step. The number of cells from the trace to the PEC box in the x and z directions are shown in the legend.

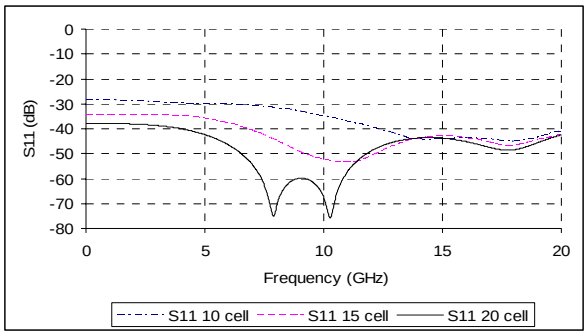

Fig. 9. Return loss for the microstrip incident on the Floating PML for differently sized PEC boxes.

IV. APPLICATIONS

In this section we examine two practical applications of the Floating PML: the microstrip-fed slot antenna, and the dual band dual slot stripline antenna.

A. Microstrip-Fed Slot Antenna

The microstrip slot antenna to be studied is shown in Fig. 10. This problem is particularly problematic for termination of the microstrip line because the impedance match is very narrow, leading to a large reflected pulse with long duration and interaction with the PML. In this example a Floating PML was used to obtain results that were similar to the published results for the antenna pattern [12]. In the published results, the microstrip line is terminated in a lumped element instead of a Floating PML.

As we can see from the results in Fig. 11, the return loss using the Floating PML matched simulated results using the Lumped Load method [13], as well as measured results [13].

In Fig. 12, we show that the antenna pattern matched the measured pattern and the pattern simulated using the LE-FDTD method.

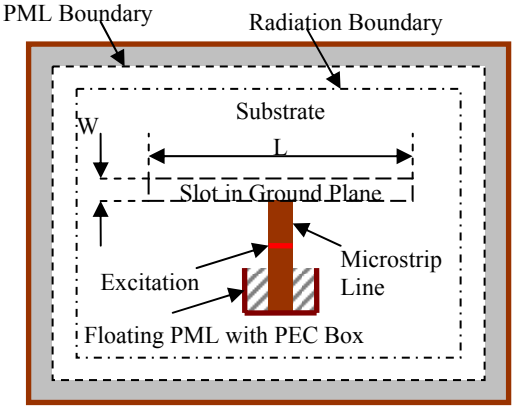

Fig. 10. The microstrip-fed slot antenna.

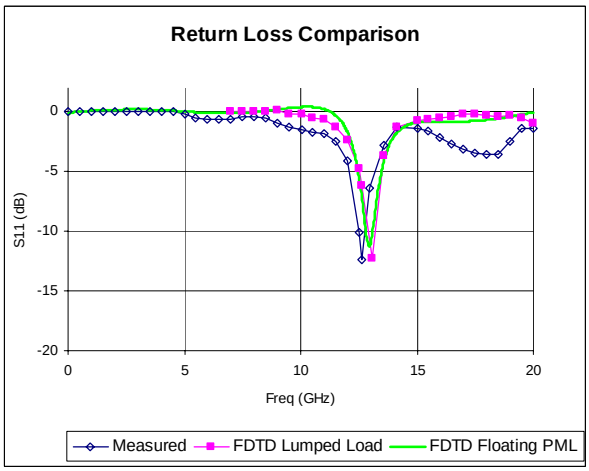

Fig. 11. Return loss comparison between the Lumped load method as in [13], the Floating PML, and measured [13] results.

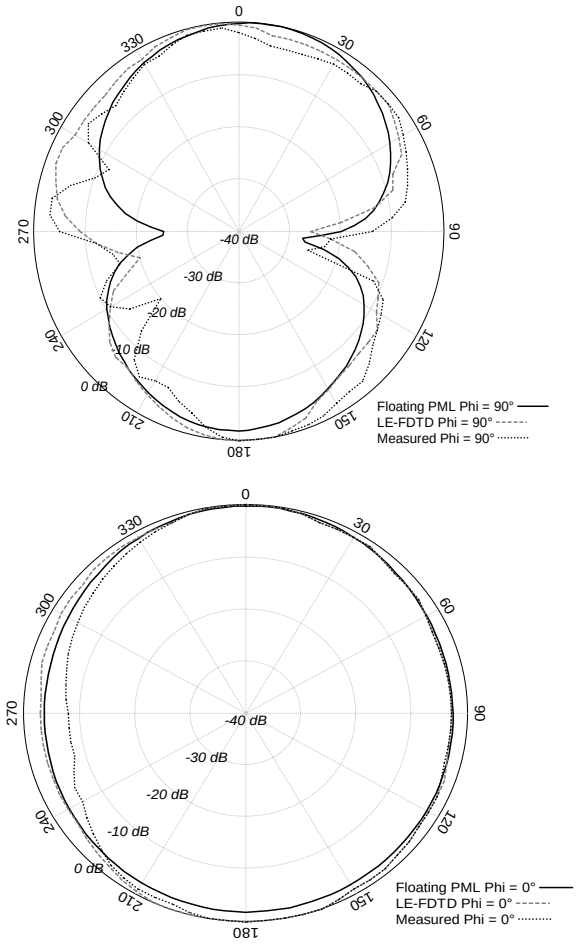

Fig. 12. Measured [12], LE-FDTD simulated [12], and Floating PML simulated antenna patterns at 13 GHz for simple slot antenna along Phi = 0 (X-Z Plane) and Phi = 90 (Y-Z Plane).

B. Dual Band Dual Slot Stripline Antenna

In this example we examine a stripline application [14] for the Floating PML as shown in Fig. 13. The stripline is used to feed dual slots which act as a single antenna with dual bands. The stripline is excited on both sides of the trace, as shown in Fig. 14. The dimensions are given in Table 1. The pulse travels in both directions, where on one side the pulse is absorbed by the Floating PML and the pulse continues to travel towards the dual slots.

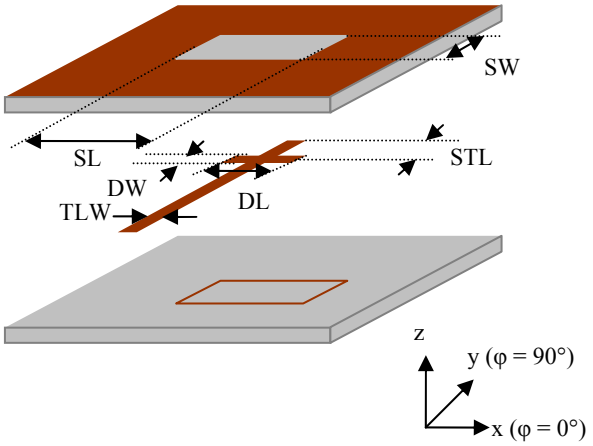

Fig. 13. The dual band dual slot stripline antenna [14]. (for dimensions see Table 1).

Table 1. Dual slot stripline antenna dimensions.

Dimension	Size (cells)	Physical Size (mm)	Description
TLW	8	2.6	Width of transmission line
STL	17	4.25	Stub length
SW	56	14	Width of slot
SL	120	39	Length of slot
h	5	1.575	Height of each substrate
DL	16	5.2	Length of tuning stub
DW	4	1.0	Width of tuning stub

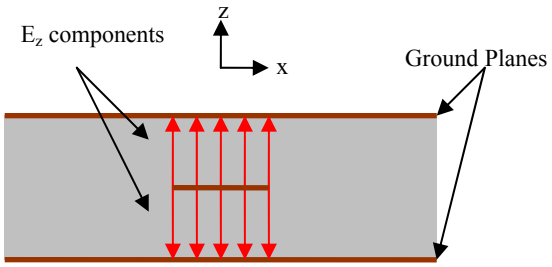

Fig. 14. Excitation of stripline structure.

In Fig. 15, we can see that the return loss of the Floating PML matches the return loss calculated using Ansoft Designer and measured results.

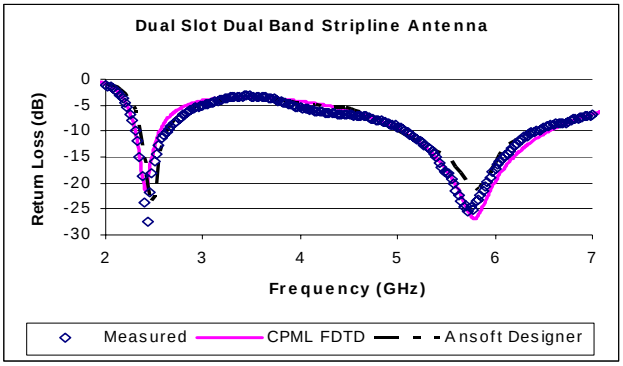

Fig. 15. Simulated return loss of dual band dual slot stripline antenna [14].

In Figs. 16 and 17, we show both the antenna co- and cross-polarization patterns at 2.45 GHz and 5.2 GHz, respectively. The results based on the Floating PML match those of the measured antenna. At both frequencies, it is noticed that E-plane cross-polarization is less than -40 dB.

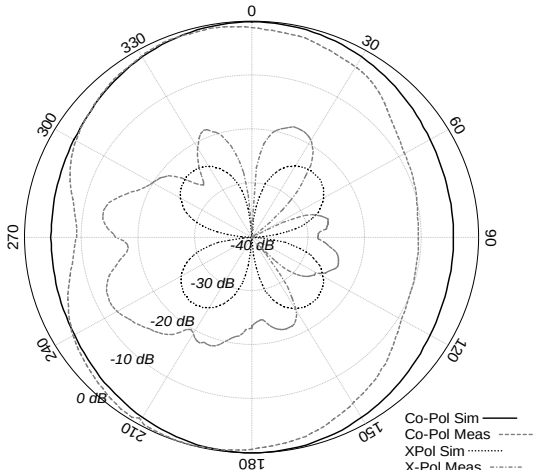

Fig. 16a. Antenna patterns at 2.45GHz: φ = 0° H-Plane.

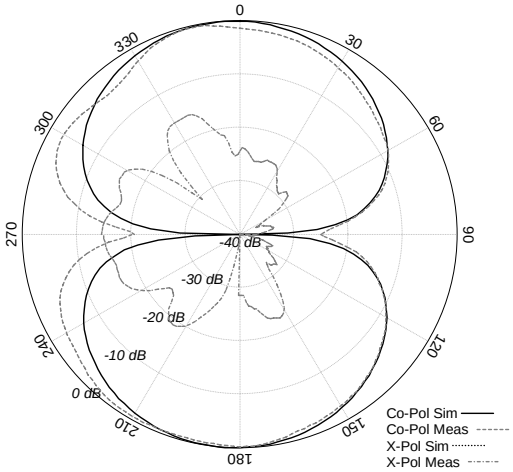

Fig. 16b. Antenna patterns at 2.45 GHz, φ=90° E-Plane.

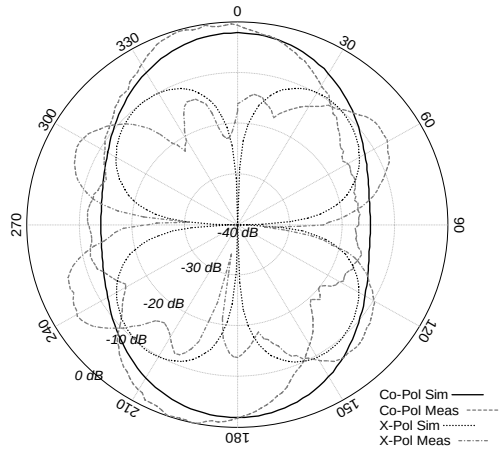

Fig. 17a. Antenna patterns at 5.8 GHz: φ = 0° H-Plane.

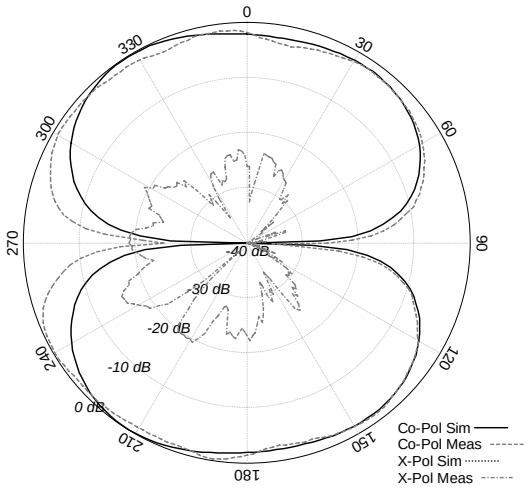

Fig. 17b. Antenna patterns at 5.8 GHz: φ = 90° E-Plane.

V. CONCLUSION

In this paper, the Floating PML, a new application for the CPML is introduced and discussed. Two benchmark cases to measure the return loss performance of the proposed Floating PML are considered for stripline and microstrip structures. Numerical results for microstrip-fed slot and for a dual band dual slot stripline antenna supporting the optimized CPML formulation and the Floating PML are then presented. In the Appendix we discuss the implementation of an optimized version of the CPML, where the κ tensor parameters (PML coefficients) have been removed from the main FDTD equations. It is successfully shown that it is possible to implement the Floating PML within the solution space as a port, as long as it is surrounded by a PEC box, meaning it is closed on five of the six sides of the box.

REFERENCES

[1] Y. Zhang and S.-W. Lu, "Genetic algorithm in reduction of numerical dispersion of 3-D alternating-direction-implicit finite-difference time-domain method," *IEEE Trans. on Microwave Theory and Techniques*, vol. 55, no. 5, pp. 966 - 973, May 2007.

[2] C.-C. Wang and C.-W. Kuo, "An efficient scheme for processing arbitrary lumped multiport devices in the finite-difference time-domain method," *IEEE Trans. on Microwave Theory and Techniques*, vol. 55, no. 5, pp. 958 – 965, May 2007.

[3] A. Taflove and S. C. Hagness, *Computational Electrodynamics The Finite-Difference Time-Domain Method*, Third Edition, Artech House, 2005.

[4] D. M. Sheen, S. M. Ali, M. D. Abouzahra, and J. A. Kong, "Application of the three-dimensional finite-difference time-domain method to the analysis of planar microstrip circuits," *IEEE Trans. on Microwave Theory and Techniques,* vol. 38, no. 7, pp. 849 – 857, July 1990.

[5] R. J. Luebbers and H. S. Langdon, "A simple feed model that reduces time steps needed for FDTD antenna and microstrip calculations," *IEEE Trans. on Antennas and Propagation*, vol. 44, no. 7, pp. 1000 – 1005, July 1996.

[6] J. W. Schuster, R. J. Luebbers, and T. G. Livernois, "Application of the recursive convolution technique to modeling lumped circuit elements in FDTD simulations," *IEEE Antennas and Propagation Society International Symposium*, vol. 4, pp. 1792 – 1795, 21-26 June 1998.

[7] M. Piket-May, A. Taflove, and J. Baron, "FD-TD modeling of digital signal propagation in 3-D circuits with passive and active loads," *IEEE Trans. on Microwave Theory and Techniques*, vol. 42, no. 8, pp. 1514 – 1523, August 1994.

[8] J. A. Pereda, F. Alimenti, P. Mezzanotte, L. Roselli, and R. Sorrentino, "A new algorithm for the incorporation of arbitrary linear lumped networks into FDTD simulators," *IEEE Trans. on Microwave Theory and Techniques*, vol. 47, no. 6, Part 2, pp. 943 – 949, June 1999.

[9] M. Wong and A. R. Sebak, "The Floating PML: a novel CPML application," *ANTEM/URSI Conference Ecole Polytechnqiue*, Montreal, QC, Canada, pp. 601, 17-19 July 2006.

[10] S. D. Gedney, "An anisotropic PML absorbing media for FDTD simulation of fields in lossy dispersive media," *Electromagnetics*, vol. 16, pp. 399-415, 1996.

[11] M. Wong, B. M. Hobson, and A. R. Sebak, "A coaxial to waveguide feeding method for substrate integrated waveguides," *EMTS 2007 International URSI – Commission B Electromagnetic Theory Symposium*, Fairmount Chateau Laurier, Ottawa, 26-28 July 2007.

[12] M. Cryan, S. Helbing, F. Alimenti, P. Mezzanotte, L. Roselli, and R. Sorrentino, "Analysis and design of quasi-optical multipliers using lumped element (LE)-FDTD method," *IEEE Antennas and Propagation Society International Symposium*, vol. 1, pp. 100 - 103, 11-16 July 1999.

[13] M. Cryan, S. Helbing, F. Alimenti, P. Mezzanotte, L. Roselli, and R. Sorrentino, "Analysis and design of quasi-optical multipliers using lumped element (LE)-FDTD method," *IEEE Antennas and Propagation Society International Symposium*, vol. 1, pp. 100 -103, 11-16 July 1999.

[14] M. Wong, A. R. Sebak, and T. A. Denidni, "Analysis of a Dual-Band Dual Slot omnidirectional stripline antenna," *IEEE Antennas and Wireless Propagation Letters*, vol. 6, pp. 199 - 202, 2007.

APPENDIX A: AN OPTIMIZED CPML FORMULATION: ISOLATION OF CPML COEFFICIENTS

The CPML formulation is very efficient in its implementation due to the fact that the recursively calculated CPML components (see equation (2)) need only be calculated and added to the individual vector components within the PML [3]. Conversely, the Uniaxial Perfectly Matched Layer (UPML) requires the computation of the PML components throughout the entire solution space, requiring a much larger amount of computation time [3].

The complex frequency shifted (CFS) tensor allows the CPML to absorb waves of low frequency or long duration, since the denominator does not approach zero at DC [3]. It is given as,

$$s_w = \kappa_w + \frac{\sigma_w}{a_w + j\omega\varepsilon}. \qquad (1)$$

The "a" term in the denominator is added to prevent the denominator from approaching zero when the radian frequency "ω" approaches zero and has no physical significance. "ε" and "σ" are properties of the material. "κ" has a value of 1.0 throughout the solution space, however, these κ coefficients can be greater than 1.0 in the CPML region to effectively scale the mesh so that at incoming wave is more effectively attenuated [3]. The subscripts w and v represent vectors perpendicular to the wave propagation.

The recursively calculated CPML component using the CFS tensor in equation (1) is given as [10],

$$\psi_{w,v}(n) = b_w \psi_{w,v}(n-1) + c_w \frac{\partial}{\partial w} H_v(n) \qquad (2)$$

where

$$b_w = \exp\left[-\left(\frac{\sigma_w}{\varepsilon_o \kappa_w} + \frac{a_w}{\varepsilon_o}\right)\Delta t\right],$$

$$c_w = \frac{\sigma_w}{\sigma_w \kappa_w + \kappa_w^2 a_w}\left[\exp\left[-\left(\frac{\sigma_w}{\varepsilon_o \kappa_w} + \frac{a_w}{\varepsilon_o}\right)\Delta t\right] - 1\right].$$

As discussed above, the κ tensor parameters as given in equation (1) and implemented in the CPML in equation (2) have a value of 1.0 throughout the main solution space, however, still appear within the standard CPML formulation as shown in equation (3) [10]. If left in this format, the software needs to either store values of κ = 1.0 throughout the solution space, or check to see if the computation lies within the PML to compute a set of FDTD equations without the κ component.

In this section we present a solution to this problem. It is possible to remove the κ component from the CPML FDTD in equation (3), to reduce storage requirements or simplify the programming, depending on the implementation. The equations within the FDTD computation region then reduce to the standard Yee equations. This yields optimal simplicity / accuracy within the computational region and increases running speed / reduces storage at the same time.

Consider the standard E field updates equation in the CPML region,

$$E_x\Big|_{i+1/2,j,k}^{n+1/2} = C_{ax}\Big|_{i+1/2,j,k} Ex\Big|_{i+1/2,j,k}^{n-1/2} + C_{bx}\Big|_{i+1/2,j,k} \left(\begin{array}{l} \dfrac{H_z\Big|_{i+1/2,j+1/2,k}^{n} - H_z\Big|_{i+1/2,j-1/2,k}^{n}}{\kappa_{yj}\Delta y} - \\ \dfrac{H_y\Big|_{i+1/2,j,k+1/2}^{n} - H_y\Big|_{i+1/2,j,k-1/2}^{n}}{\kappa_{zk}\Delta z} \\ + \psi_{Ex,y}\Big|_{i+1/2,j,k}^{n} - \psi_{Ex,z}\Big|_{i+1/2,j,k}^{n} \end{array} \right). \qquad (3)$$

Without loss of generality, this may be written as

$$E_x\Big|_{i+1/2,j,k}^{n+1/2} = C_{ax}\Big|_{i+1/2,j,k} Ex\Big|_{i+1/2,j,k}^{n-1/2} + C_{bx}\Big|_{i+1/2,j,k} \left(\begin{array}{l} \left[\begin{array}{l} \dfrac{H_z\Big|_{i+1/2,j+1/2,k}^{n} - H_z\Big|_{i+1/2,j-1/2,k}^{n}}{\Delta y} - \\ \dfrac{H_z\Big|_{i+1/2,j+1/2,k}^{n} - H_z\Big|_{i+1/2,j-1/2,k}^{n}}{\Delta y} \end{array} \right] \\ + \dfrac{H_z\Big|_{i+1/2,j+1/2,k}^{n} - H_z\Big|_{i+1/2,j-1/2,k}^{n}}{\kappa_{yj}\Delta y} \\ - \left[\begin{array}{l} \dfrac{H_y\Big|_{i+1/2,j,k+1/2}^{n} - H_y\Big|_{i+1/2,j,k-1/2}^{n}}{\Delta z} - \\ \dfrac{H_y\Big|_{i+1/2,j,k+1/2}^{n} - H_y\Big|_{i+1/2,j,k-1/2}^{n}}{\Delta z} \end{array} \right] \\ - \dfrac{H_y\Big|_{i+1/2,j,k+1/2}^{n} - H_y\Big|_{i+1/2,j,k-1/2}^{n}}{\kappa_{zk}\Delta z} \\ + \psi_{Ex,y}\Big|_{i+1/2,j,k}^{n} - \psi_{Ex,z}\Big|_{i+1/2,j,k}^{n} \end{array} \right). \quad (4)$$

Notice that the two identical difference terms in equation (4) have been added and subtracted.

Consider now, grouping the second two components and factoring out the difference term,

$$E_x\Big|_{i+1/2,j,k}^{n+1/2} = C_{ax}\Big|_{i+1/2,j,k} Ex\Big|_{i+1/2,j,k}^{n-1/2} + C_{bx}\Big|_{i+1/2,j,k} \left(\begin{array}{l} \dfrac{H_z\Big|_{i+1/2,j+1/2,k}^{n} - H_z\Big|_{i+1/2,j-1/2,k}^{n}}{\Delta y} + \\ \left[\dfrac{1}{\kappa_{yj}} - 1 \right] \dfrac{H_z\Big|_{i+1/2,j+1/2,k}^{n} - H_z\Big|_{i+1/2,j-1/2,k}^{n}}{\Delta y} \\ \dfrac{H_y\Big|_{i+1/2,j,k+1/2}^{n} - H_y\Big|_{i+1/2,j,k-1/2}^{n}}{\Delta z} \\ - \left[\dfrac{1}{\kappa_{zk}} - 1 \right] \dfrac{H_y\Big|_{i+1/2,j,k+1/2}^{n} - H_y\Big|_{i+1/2,j,k-1/2}^{n}}{\Delta z} \\ + \psi_{Ex,y}\Big|_{i+1/2,j,k}^{n} - \psi_{Ex,z}\Big|_{i+1/2,j,k}^{n} \end{array} \right). \quad (5)$$

If the κ components are 1.0 within the main solution space, the new terms disappear, yielding the standard Yee update equations. The new terms, then, can be added within the PML only. The finite difference update equation for the Ex component is then,

$$E_x\Big|_{i+1/2,j,k}^{n+1/2} = C_{ax}\Big|_{i+1/2,j,k} Ex\Big|_{i+1/2,j,k}^{n-1/2} + C_{bx}\Big|_{i+1/2,j,k} \left(\begin{array}{l} \dfrac{H_z\Big|_{i+1/2,j+1/2,k}^{n} - H_z\Big|_{i+1/2,j-1/2,k}^{n}}{\Delta y} - \\ \dfrac{H_y\Big|_{i+1/2,j,k+1/2}^{n} - H_y\Big|_{i+1/2,j,k-1/2}^{n}}{\Delta z} \end{array} \right). \quad (6)$$

This difference equation may now be calculated within the entire solution space, including the PML, in one loop. Within the PML, the ψ components are then added after computation of equation (4), along with the new difference terms, as follows,

$$E_{xPML}\Big|_{i+1/2,j,k}^{n+1/2} = E_x\Big|_{i+1/2,j,k}^{n+1/2} + C_{bx}\Big|_{i+1/2,j,k} \left(\begin{array}{l} \left[\dfrac{1-\kappa_{yj}}{\kappa_{yj}} \right] \dfrac{H_z\Big|_{i+1/2,j+1/2,k}^{n} - H_z\Big|_{i+1/2,j-1/2,k}^{n}}{\Delta y} \\ - \left[\dfrac{1-\kappa_{zk}}{\kappa_{zk}} \right] \dfrac{H_y\Big|_{i+1/2,j,k+1/2}^{n} - H_y\Big|_{i+1/2,j,k-1/2}^{n}}{\Delta z} \\ + \psi_{Ex,y}\Big|_{i+1/2,j,k}^{n} - \psi_{Ex,z}\Big|_{i+1/2,j,k}^{n} \end{array} \right). \quad (7)$$

This completes the modified formulation of the CPML. We can now assign a PEC wall around the entire solution space, then implement equation (6) everywhere, including the PML region. We then add the PML material in the regions required as described by equation (7).

Note that for this implementation, 2 additional add/subtracts and 1 additional multiplication must take place in equations (6) and (7) as compared to equation (3). One additional "if then" is saved per field or cell, depending on the implementation.

Michael Wong received the B.Sc. degree in Electrical Engineering from Queen's University in Kingston, Ontario, in 1997, and the M.Sc. degree in Electrical Engineering from Concordia University in Montreal, Quebec in 2006. He is currently a Ph.D. candidate at Concordia University in Montreal, Quebec. From 1998 to 2004 he was with TMI Communications (later Mobile Satellite Ventures) working on software, RF Engineering, licensing, and regulatory requirements all related to satellite communications and mobile satellite telephony. His current research focuses on electromagnetic band gap structures for antenna and microwave device applications, stripline and microstrip antennas, as well as the FDTD method.

Abdel-Razik Sebak received the B.Sc. degree (with honors) in Electrical Engineering from Cairo University, Egypt, in 1976 and the B.Sc. degree in Applied Mathematics from Ein Shams University, Egypt, in 1978. He received the M.Eng. and Ph.D. degrees from the University of Manitoba, Winnipeg, MB, Canada, in 1982 and 1984, respectively, both in electrical engineering. From 1984 to 1986, he was with the Canadian Marconi Company, Kanata, Ontario, working on the design of microstrip phased array antennas. From 1987 to 2002, he was a Professor in the Electrical and Computer Engineering Department, University of Manitoba, Winnipeg. He is currently a Professor of Electrical and Computer Engineering, Concordia University, Montreal. His current research interests include phased array antennas, computational electromagnetics, integrated antennas, electromagnetic theory, interaction of EM waves with new materials and bio-electromagnetics. Dr. Sebak received the 2003-2004 Faculty of Engineering, Concordia University double Merit Award for outstanding Teaching and Research. He has also received the 2000 and 1992 University of Manitoba Merit Award for outstanding Teaching and Research, the 1994 Rh Award for Outstanding Contributions to Scholarship and Research in the Applied Sciences category, and the 1996 Faculty of Engineering Superior Academic Performance. Dr. Sebak has served as Chair for the IEEE Canada Awards and Recognition Committee (2002-2004) and IEEE Canada CONAC (1999-2001). He has also served as Chair of the IEEE Winnipeg Section (1996-97). He is the Technical Program Co-Chair (2006) and served as the Treasurer (1992, 1996, and 2000) and Publicity Chair (1994) for the Symposium on Antenna Technology and Applied Electromagnetics (ANTEM). Dr. Sebak has also served as Chair (1991-92) of the joint IEEE AP/MTT/VT Winnipeg Chapter. He received, as the Chapter Chair, the 1992 IEEE Antennas and Propagation Society Best Chapter Award. He is a Senior Member of the IEEE, and a member of the International Union of Radio Science Commission B.